

# Estimation of Rotor Type Using Ferrite Magnet Considering the Magnetization Process

Kyu-Seob Kim, Min-Ro Park, Hae-Joong Kim, Seung-Hee Chai, and Jung-Pyo Hong, *Senior Member, IEEE*

Department of Automotive Engineering, Hanyang University, Seoul 133-791, Korea

This paper deals with the post assembly magnetization process of motors using ferrite permanent magnets. In order to meet the needs of mass production, most motors are magnetized post assembly. However, increasingly complex shapes are required to maximize the flux of permanent magnets. As a result, certain locations in the magnet are not fully magnetized by the magnetizing fixture due to insufficient magnetomotive force. Therefore, an analysis concerning the post assembly magnetization is needed. In this paper, the concentrated flux spoke type synchronous motor is analyzed to magnetization process, and then the magnetization level is compared by linkage flux value between post assembly and fully magnetization. Finally, back electromotive force is estimated by post assembly magnetization method the according to the magnet shape.

**Index Terms**— Ferrite magnet, magnetization level, magnetization processes, magnetizing fixture, post assembly magnetization

## I. INTRODUCTION

RECENTLY ENVIRONMENTAL issues have worsened, and the depletion of fossil fuels has accelerated. To alleviate these problems, motors with much higher efficiency are required [1]-[3]. One particular type of motor, the interior permanent magnet synchronous motor (IPMSM), is widely used to meet the demand of high power density, with rare earth permanent magnets (PM) frequently being essentially incorporated [4].

However, the rare earth permanent magnet is both costly and sparse. The rarity of the PM subsequently generates imbalances in supply and increases in price. Therefore, new types of motor have been proposed to eliminate the need for rare earth materials, without sacrificing performance. Concentrated flux spoke type motors, using ferrite PMs, are particularly attractive. In this type of motor, in order to increase the flux of the ferrite magnet, the magnet's shape and arrangement become increasingly complex. For obtaining the motor performance as designed, magnet quality must be guaranteed. In the mass production system, the post assembly magnetization method is used. As a result, certain locations in the magnet are partially magnetized. Therefore, magnet shape and arrangement are the important [5].

In this paper, the post assembly magnetization method is analyzed with respect to the concentrated flux spoke type motor including the various magnet shape. According to this process, the non-magnetized PMs are installed on various rotor core.

The rotor and stator are combined after discharging current flows into the magnetizing fixture and rotor with PM. According to the magnet shape, the back EMF and magnetization level are calculated by finite element method (FEM).

## II. PM PERFORMANCE ACCORDING TO MAGNETIC FIELD INTENSITY

The PMs can be either isotropic or anisotropic, depending on the production method. Generally, the residual flux density of anisotropic PMs is higher than that of isotropic PMs. In the anisotropic PM, the hard axis along a non-preferred direction is

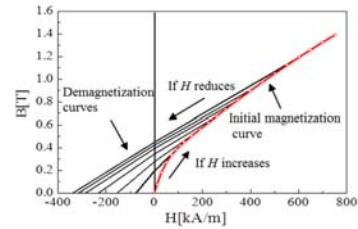


Fig. 1. B-H curve of magnets during magnetization field intensity.

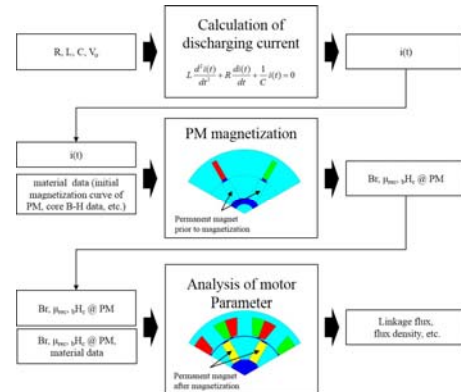


Fig. 2. Post assembly magnetization process.

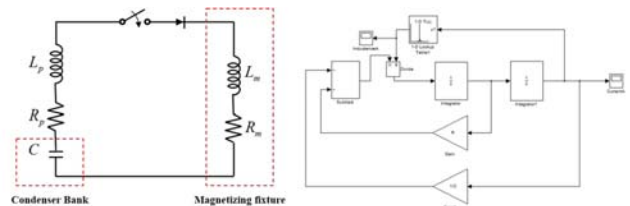


Fig. 3. Magnetizing fixture circuit with condenser bank and block diagram.

assumed to be linear. The preferred direction shows the nonlinear performance in the easy axis. The PM materials along the easy axis have a nonlinear B-H curve as shown in Fig. 1. In the magnetizing force  $H=0$  and flux density  $B=0$ , this is the initial point of the non-magnetized magnet. During the magnetization process, when  $H$  increases,  $B$  will increase along the initial magnetization curve. When  $H$  decreases,  $B$  will decrease along the demagnetization curve. If  $H$  is not sufficient,  $B$  cannot reach the saturation point. Therefore, when  $H=0$ ,  $B_r$  is lower than fully saturated. Additionally, during this time, coercive force drops and recoil permeability grows. All of these

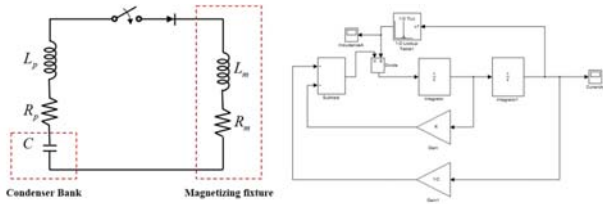


Fig. 3. Magnetizing fixture circuit with condenser bank and block diagram.

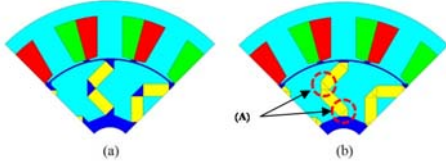


Fig. 4. FEM modeling (a) rectangular magnet shape (b) hexagon magnet shape

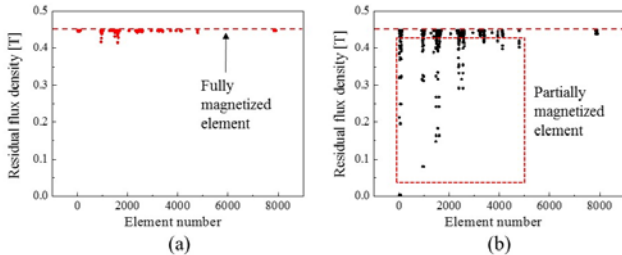


Fig. 5. Residual flux density according to element number in the PM (a) rectangular magnet shape (b) hexagon magnet shape diagram.

various effects ultimately influence the motor's performance. Therefore, during the post assembly magnetization procedure proper magnet shape and arrangement provide for sufficient magnetic field intensity.

### III. POST ASSEMBLY MAGNETIZATION PROCESS

In mass production, productivity is influenced by product state. The magnet's shape is an important factor that is related to the motor's performance. In this paper, magnetization level and back EMF are studied in post assembly magnetization according to the PM shape. Fig.2 shows the post assembly magnetization process. The circuit is governed by the following

$$L \frac{d^2 i(t)}{dt^2} + R \frac{di(t)}{dt} + \frac{1}{C} i(t) = 0 \quad (1)$$

where  $L=L_p+L_m$ ,  $R=R_p+R_m$ , resistance,  $C$  is the capacitance of the condenser bank,  $i(t)$  is the current flowing into the magnetizing fixture. This equation is solved by MATLAB Simulink which is shown Fig.3 [6].

### IV. ANALYSIS MODEL

In this paper, the models are estimated to various type according to back EMF and magnetization level. The magnetization level is calculated by following equation.

$$\text{magnetizaion level(\%)} = \frac{\text{linkage flux@partially magnetizaiton}}{\text{linkage flux@fully magnetizaiton}} \times 100 \quad (2)$$

Fig. 4 shows two of the analysis models. This motor is the concentrated flux spoke type using ferrite PM. The PM is hexagonally shaped, which maximizes the flux given the limited width. Although sufficient discharging current flows into the magnetizing fixture, the edge of PM (A) may be partially magnetized. Therefore, in this case the magnetization level is lower than fully magnetization.

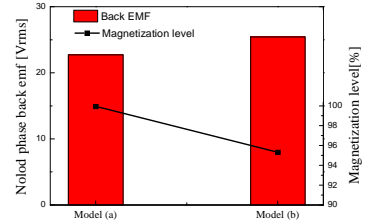


Fig. 6. Results of noload back EMF and magnetization level in model (a),

## V. RESULT AND CONCLUSION

Fig. 5 shows residual flux density according to element number. The flux density of the rectangular magnet (a) is distributed to 0.447 T, which is the fully magnetized level. However, the flux density of the hexagonal magnet (b) ranges from 0 to 0.447 T. Table II shows the mean and standard deviation concerning tow case. The standard deviation of model (b) is larger than model (a). However, the mean value of model (b) is not much lower than model (a), because the magnet area is larger than the edge area.

The back EMF and magnetization level are shown in Fig. 6. The magnetization level is calculated by post assembly magnetization divided by full magnetization. The level of model (a) is 99.93%, model (b) is 95.32%. The magnetization level of model (b) result from the edge which is not fully magnetized. Although the model (b) is not fully magnetized, the model (b) of back EMF is higher than the model (a). In the full paper, various type is estimated by analyzing the back EMF and magnetization level, and the proper type will be introduced.

### ACKNOWLEDGMENT

This research was supported by the MKE (The Ministry of Knowledge Economy), Korea, under the CITRC (Convergence Information Technology Research Center) support program (NIPA-2013-H0401-13-1008) supervised by the NIPA (National IT Industry Promotion Agency).

This work supported by a research program (The Specialized Research Center on the Future Ground System) funded by the Agency for Defense Development of Korea and we appreciate it.

### REFERENCES

- [1] M. F. Hsieh, Y. M. Lien, and D. G. Dorrell, "Post-Assembly Magnetization of Rare-Earth Fractional-Slot Surface Permanent-Magnet Machines Using a Two-Shot Method," *IEEE Trans. on Ind. Appl.*, vol. 47, pp. 2478-2486, 2011.
- [2] B. H. Lee, K. S. Kim, J. W. Jung, J. P. Hong and Y. K. Kim, "Temperature Estimation of IPMSM Using Thermal Equivalent Circuit," *IEEE Trans. on Magn.*, vol. 48, pp. 2949-2952, 2012.
- [3] S. J. Lee, K. S. Kim, S. Cho, J. Jang, T. Lee and J. P. Hong, "Optimal design of interior permanent magnet synchronous motor considering the manufacturing tolerances using Taguchi robust design," *IET. Electr. Power Appl.*, vol. 8, pp. 23-28, 2014.
- [4] K. S. Kim, B. H. Lee, J. W. Jung and J. P. Hong, "Thermal Analysis of Water Cooled ISG Based on a Thermal Equivalent Circuit Network," *J. Electr. Eng. Technol.*, vol. 9, pp. 893-898, 2014.
- [5] D. G. Dorrell, M.F. Hsieh, and Y. C. Hsu, "Post Assembly Magnetization Patterns in Rare-Earth Permanent-Magnet Motors," *IEEE Trans. on Magn.*, vol. 43, pp. 2489-2491, 2007.
- [6] J. K. Lee, "The Analysis of a Magnetizing Fixture for a Multipole Nd-Fe-B Magnet," *IEEE Trans. on Magn.*, vol. 24, pp. 2166-2171, 1988.